

An  $S = 2$  Cyanide-Bridged Trinuclear  $\text{Fe}^{\text{III}}_2\text{Ni}^{\text{II}}$  Single-Molecule MagnetDongfeng Li,<sup>†</sup> Rodolphe Clérac,<sup>\*‡</sup> Sean Parkin,<sup>†</sup> Guangbin Wang,<sup>§</sup> Gordon T. Yee,<sup>§</sup> and Stephen M. Holmes<sup>\*†</sup>

Department of Chemistry, University of Kentucky, Lexington, Kentucky 40506-0055, Centre de Recherche Paul Pascal, UPR-CNRS 8641, 115 avenue du Dr. A. Schweitzer, 33600 Pessac, France, and Department of Chemistry, Virginia Polytechnic Institute and State University, Blacksburg, Virginia 24061

Received March 7, 2006

Treatment of  $[\text{NEt}_4][(\text{pzTp})\text{Fe}^{\text{III}}(\text{CN})_3]$  (**1**) with  $\text{Ni}^{\text{II}}(\text{OTf})_2$  ( $\text{OTf} =$  trifluoromethanesulfonate) and 1,5,8,12-tetraazadodecane (**L**) affords  $\{[(\text{pzTp})\text{Fe}^{\text{III}}(\text{CN})_3]_2[\text{Ni}^{\text{II}}(\text{L})]\} \cdot \frac{1}{2}\text{MeOH}$  (**2**), while 2,2'-bipyridine (**bipy**) affords  $\{[(\text{pzTp})\text{Fe}^{\text{III}}(\text{CN})_3]_2[\text{Ni}^{\text{II}}(\text{bipy})_2]\} \cdot 2\text{H}_2\text{O}$  (**3**). Magnetic measurements indicate that **2** and **3** have  $S = 2$  ground states and that **3** exhibits slow relaxation of the magnetization above 2 K.

The burgeoning field of single-molecule magnet (SMM) materials has seen extensive activity over the past decade. These inorganic complexes exhibit superparamagnetic-like behavior owing to the large spin ground state ( $S$ ) and Ising-type anisotropy ( $D < 0$  and small  $E$ ) derived from the transition-metal centers used in their construction.<sup>1</sup> These characteristics create an energy barrier ( $\Delta$ ) between the two thermodynamically equivalent  $m_S = \pm S$  configurations. Hence, below  $T_B$ , the so-called blocking temperature, the thermal energy is insufficient to overcome  $\Delta$  and the spin is trapped in one of the two configurations. Application of large magnetic fields ( $H_{\text{dc}}$ ) saturates the magnetization ( $M$ ) of the sample, and removal of this field ( $H_{\text{dc}} = 0$ ) will induce a slow decay of  $M$  toward zero with a characteristic relaxation time ( $\tau$ ). The relaxation time usually exhibits thermally activated behavior and can be measured using the time dependence of  $M$  or, more commonly, the frequency ( $\nu$ ) dependence of the ac susceptibility. At very low temperatures, quantum tunneling of the magnetization (QTM) often relaxes the magnetization at rates faster than thermally activated pathways. Experimentally, a crossover occurs between these two regimes, and in this intermediate temperature range, the thermal barrier ( $\Delta$ ) is circumvented by quantum tunneling, affording an effective barrier  $\Delta_{\text{eff}}$ .<sup>1</sup>

While the vast majority of SMMs are derived from metal centers linked by oxo and carboxylate ligands, several groups

have recently described that such complexes can also be prepared from  $[\text{fac-L}^m\text{M}^n(\text{CN})_3]^{n+m-3}$  units.<sup>2</sup> The preparation of these cyanometalate complexes utilizes a building-block synthetic approach, where discrete molecular precursors are allowed to self-assemble into a common structural archetype, allowing for detailed structure–property relationships to be described. As part of a continuing effort to develop structurally related cyanometalate SMMs, we recently developed a series of poly(pyrazolylborate) cyanometalate building blocks and have systematically investigated the controlled aggregation of these units into complexes and networks.<sup>3</sup> Herein, we report on the synthesis, structures, and spectroscopic and magnetic properties of two trinuclear  $\text{Fe}^{\text{III}}_2\text{Ni}^{\text{II}}$  complexes,  $\{[(\text{pzTp})\text{Fe}^{\text{III}}(\text{CN})_3]_2[\text{Ni}^{\text{II}}(\text{L})]\} \cdot \frac{1}{2}\text{MeOH}$  (**2**;  $\text{L} = 1,5,8,12$ -tetraazadodecane) and  $\{[(\text{pzTp})\text{Fe}^{\text{III}}(\text{CN})_3]_2[\text{Ni}^{\text{II}}(\text{bipy})_2]\} \cdot 2\text{H}_2\text{O}$  (**3**;  $\text{bipy} = 2,2'$ -bipyridine), of which the latter exhibits slow relaxation of the magnetization above 2 K.

Treatment of  $[\text{NEt}_4][(\text{pzTp})\text{Fe}^{\text{III}}(\text{CN})_3]$  (**1**) with nickel(II) trifluoromethanesulfonate and 1,5,8,12-tetraazadodecane (**L**) or 2,2'-bipyridine (**bipy**) in methanol cleanly affords red **2** and orange **3** as crystalline solids.<sup>3c,4,5</sup> The infrared spectra exhibit intense  $\nu_{\text{CN}}$  stretching absorptions at 2137 and 2122  $\text{cm}^{-1}$  for **2** and at 2162 and 2119  $\text{cm}^{-1}$  for **3** that are tentatively assigned as bridging and terminal cyanides, respectively.<sup>3</sup>

Compound **2** crystallizes in the triclinic  $P\bar{1}$  space group.<sup>4,5</sup> The neutral complex consists of a central octahedral  $[\text{Ni}^{\text{II}}(\text{L})]^{2+}$  unit that is linked to two  $[(\text{pzTp})\text{Fe}^{\text{III}}(\text{CN})_3]^-$  anions (Figure 1), via bridging cyanides, that are axial to the coordinated 1,5,8,12-tetraazadodecane ligand. The Ni–N bond distances for the *trans*-cyanides are 2.109(6) (Ni1–

\* To whom correspondence should be addressed. E-mail: smholm2@uky.edu (S.M.H.), clerac@crpp-bordeaux.cnrs.fr (R.C.).

<sup>†</sup> University of Kentucky.

<sup>‡</sup> UPR-CNRS 8641.

<sup>§</sup> Virginia Polytechnic Institute and State University.

(1) (a) Sessoli, R.; Gatteschi, D. *Angew. Chem., Int. Ed.* **2003**, *42*, 268–297 and references cited therein. (b) Beltran, L. M. C.; Long, J. R. *Acc. Chem. Res.* **2005**, *38*, 325–334 and references cited therein.

(2) (a) Schelter, E. J.; Prosvirin, A. V.; Dunbar, K. R. *J. Am. Chem. Soc.* **2004**, *126*, 15004–15005. (b) Wang, S.; Zou, J.-L.; Zhou, H.-C.; Choi, H. J.; Ke, Y.; Long, J. R.; You, X.-Z. *Angew. Chem., Int. Ed.* **2004**, *43*, 5940–5943. (c) Sokol, J. J.; Hee, A. G.; Long, J. R. *J. Am. Chem. Soc.* **2002**, *124*, 7656–7657.

(3) (a) Li, D.; Parkin, S.; Wang, G.; Yee, G. T.; Prosvirin, A. V.; Holmes, S. M. *Inorg. Chem.* **2005**, *44*, 4903–4905. (b) Li, D.; Parkin, S.; Wang, G.; Yee, G. T.; Holmes, S. M. *Inorg. Chem.* **2006**, *45*, 1951–1959. (c) Li, D.; Parkin, S.; Wang, G.; Yee, G. T.; Clérac, R.; Wernsdorfer, W.; Holmes, S. M. *J. Am. Chem. Soc.* **2006**, *128*, 4212–4215. (d) Li, D.; Parkin, S.; Wang, G.; Yee, G. T.; Holmes, S. M. *Inorg. Chem.* **2006**, *45*, 2773–2775.

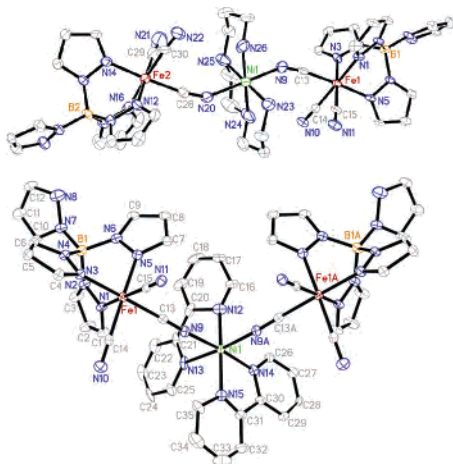


**Figure 1.** X-ray structure of **2** (top) and one structural isomer of **3** (bottom). Thermal ellipsoids are at the 50% level, and all H atoms and lattice water are eliminated for clarity. Selected bond distances (Å) and angles (deg) for **2**: Fe1–C13, 1.913(8); Fe2–C28, 1.923(8); C28–N20, 1.14(1); Ni1–N9, 2.082(6); Ni1–N20, 2.109(6); Ni1–N9–C13, 150.7(6); Ni1–N20–C28, 149.2(6); N9–Ni1–N20, 179.2(3). For **3**: Fe1–C13, 1.920(5); Ni1–N9, 2.049(4); Ni1–N9–C13, 169.8(4); N9–Ni1–N9A, 90.8(2).

N20) and 2.082(6) (Ni1–N9) Å, while those for the amine range from 2.077(9) (Ni1–N24) to 2.098(9) (Ni1–N25) Å, respectively. The terminal cyanide Fe1–C bond lengths are nearly equivalent [1.933(8) and 1.932(7) Å], with the smallest value [1.913(8) Å] found for the bridging cyanide (Fe1–C13). The terminal Fe–C≡N bond angles range from 174.9(8)° (Fe2–C30–N22) to 177.9(7)° (Fe1–C14–N10), while nonlinear bridging cyanide bond angles [Fe1–C13–N9, 170.4(6)°; Fe2–C28–N20, 170.4(7)°] are found; the Ni–N≡C bond angles are also highly bent, ranging from 149.2(6)° (Ni1–N20–C28) to 150.7(6)° (Ni1–N9–C13), respectively. The intracomplex Fe1⋯Fe2, Fe1⋯Ni1, and Fe2⋯Ni1 contacts are 9.806(2), 4.900(2), and 4.910(2) Å, respectively, while the closest intercomplex contacts between the pyrazole rings and Fe<sup>III</sup> (Fe1⋯Fe1B) centers are 6.707(2) and 12.881(2) Å, respectively.

Compound **3** crystallizes as a neutral trinuclear complex in the monoclinic  $P2_1/m$  space group.<sup>4,5</sup> The complex consists of a central [Ni<sup>II</sup>(bipy)<sub>2</sub>]<sup>2+</sup> unit located on a crystallographic mirror plane that is linked to two [(pzTp)Fe(CN)<sub>3</sub>]<sup>−</sup> anions via *cis*-cyano rather than *trans*-cyano linkages (Figure 1). Symmetry considerations dictate that two structural isomers are found in a 1:1 ratio (Figure S3 in the Supporting Information) for the nonplanar,  $C_1$ -symmetric, trinuclear complex (Figure S4 in the Supporting Information).<sup>5</sup> The Ni1–N bond distance for the bridging cyanide [Ni1–N9,

2.048(4) Å] is slightly smaller than that in **2**, while those for the coordinated bipy ligands range from 2.02(2) to 2.16(2) Å. For **3**, the terminal cyanide Fe1–C distances are essentially equivalent [1.913(5) and 1.916(5) Å], while a slightly longer bond length [1.920(5) Å] is found for the bridging cyanide (Fe1–C13). The Fe1–C≡N bond angles for the terminal cyanides range from 179.2(4)° to 179.3(4)°, while the bridging cyanide [Fe1–N9–C13, 176.4(4)°] is more acute; the Ni1–N≡C (Ni1–N9–C13) bond angle is 169.8(4)° and is more linear than those in **2**. The intracomplex Fe1⋯Ni1 and Fe1⋯Fe1A contacts are 5.080(1) and 7.747(1) Å, respectively. The closest intercomplex contacts between bipy and pyrazole rings are 3.507(5) Å, while those for the Fe<sup>III</sup> (Fe1⋯Fe1B) centers are 8.536(1) Å.

The C-bound cyanides are expected to afford low-spin Fe<sup>III</sup> ( $S = 1/2$ ) centers that exhibit orbital contributions to the magnetic moment and afford  $g$  values that deviate significantly from 2.0 (ca. 2.7; see Figure S11 in the Supporting Information).<sup>2b,3,6–9</sup> The  $\chi T$  vs  $T$  data suggest that the Fe<sup>III</sup> and Ni<sup>II</sup> ( $S = 1$ ) centers in **2** are ferromagnetically coupled (Figure S5 in the Supporting Information) because the  $\chi T$  product gradually increases from 2.75 cm<sup>3</sup> K mol<sup>−1</sup> (300 K), reaching a maximum value of 3.20 cm<sup>3</sup> K mol<sup>−1</sup> at 5 K; below 5 K,  $\chi T$  decreases toward a minimum value of 2.80 cm<sup>3</sup> K mol<sup>−1</sup> at 1.82 K. On the basis of the trinuclear structure of **2**, the magnetic data have been modeled using an isotropic Heisenberg model in the weak field approximation.<sup>6</sup> Thus, the theoretical susceptibility has been deduced from the van Vleck equation considering the following Hamiltonian:  $H = -2J_1[S_1 \cdot (S_2 + S_3)]$ , where  $J_1$  is the isotropic exchange interaction between Fe<sup>III</sup> and Ni<sup>II</sup> sites and  $S_i$  is the spin operator for each metal center ( $S_1 = 1$ , Ni<sup>II</sup>;  $S_i = 1/2$ , Fe<sup>III</sup>; with  $i = 2$  and 3). When the data below 15 K are neglected to avoid the effects of intercomplex interactions and/or magnetic anisotropy, the best set of parameters obtained is  $J_1/k_B = +1.3(1)$  K and  $g_{\text{iso}} = 2.50$  (Figure S5 in the Supporting Information).<sup>5,10</sup> The magnitude of the magnetic exchange through the cyanide bridges is lower than those obtained for other tri- and tetranuclear complexes derived from tricyanoferrate(III) and -nickel(II) centers.<sup>3,6,7</sup> On the basis of the  $J_1$  value, the first excited state ( $S = 1$ ) is ca. 2.6 K above the  $S = 2$  ground state for **2** (Figure S5 in the Supporting Information). Confirmation of this ground state is obtained in the  $M$  vs  $H_{\text{dc}}$  data at 1.85 K because the magnetization is nearly saturated at 7 T, approaching a maximum value of 4.4  $\mu_B$  (Figure S6 in the Supporting Information).<sup>5</sup> ac susceptibility measurements are frequency-independent (Figure S7 in the Supporting Infor-

(4) Crystal data for **1**: C<sub>23</sub>H<sub>32</sub>BF<sub>2</sub>FeN<sub>12</sub>,  $P2_1/n$ ,  $Z = 4$ ,  $a = 10.2580(2)$  Å,  $b = 15.2386(3)$  Å,  $c = 16.9913(4)$  Å,  $\beta = 96.1396(7)^\circ$ ,  $V = 2640.8(1)$  Å<sup>3</sup>,  $R_1 = 0.0426$ ,  $wR_2 = 0.0851$ . Crystal data for **2**: C<sub>38.5</sub>H<sub>48</sub>B<sub>2</sub>Fe<sub>2</sub>N<sub>26</sub>NiO<sub>0.5</sub>,  $P1$ ,  $Z = 2$ ,  $a = 8.6821(8)$  Å,  $b = 16.683(2)$  Å,  $c = 18.355(2)$  Å,  $\alpha = 76.425(5)^\circ$ ,  $\beta = 76.377(5)^\circ$ ,  $\gamma = 87.918(5)^\circ$ ,  $V = 2511.1(4)$  Å<sup>3</sup>,  $R_1 = 0.0905$ ,  $wR_2 = 0.2453$ . Crystal data for **3**: C<sub>50</sub>H<sub>44</sub>B<sub>2</sub>Fe<sub>2</sub>N<sub>26</sub>NiO<sub>2</sub>,  $P2_1/m$ ,  $Z = 2$ ,  $a = 8.7275(2)$  Å,  $b = 22.6306(6)$  Å,  $c = 15.3268(4)$  Å,  $\beta = 105.060(1)^\circ$ ,  $V = 2923.2(1)$  Å<sup>3</sup>,  $R_1 = 0.0691$ ,  $wR_2 = 0.0854$ . Data were collected at 90.0(2) K on a Nonius Kappa CCD diffractometer (**1**) using Mo K $\alpha$  ( $\lambda = 0.71073$  Å) radiation, while **2** and **3** utilized a Bruker Proteum X8 rotating-anode diffractometer with graphite-monochromatized Cu K $\alpha$  ( $\lambda = 1.54178$  Å) radiation. Structures were solved by direct methods and refined against all data using SHELXL97.

(5) See the Supporting Information.

(6) (a) Wang, S.; Zuo, J.-L.; Zhou, H.-C.; Song, Y.; You, X.-Z. *Inorg. Chim. Acta* **2005**, 358, 2101–2106. (b) Wang, S.; Zuo, J.-L.; Zhou, H.-C.; Song, Y.; Gao, S.; You, X.-Z. *Eur. J. Inorg. Chem.* **2004**, 3681–3687.

(7) Yang, J. Y.; Shores, M. P.; Sokol, J. J.; Long, J. R. *Inorg. Chem.* **2003**, 42, 1403–1419.

(8) Lescouëzec, R.; Vaissermann, J.; Lloret, F.; Julve, M.; Verdager, M. *Inorg. Chem.* **2002**, 41, 5943–5945.

(9) Kim, J.; Han, S.; Cho, I.-K.; Choi, K. Y.; Heu, M.; Yoon, S.; Suh, B. J. *Polyhedron* **2004**, 23, 1333–1339.

(10) Note that consideration of the intercomplex interactions in the frame of the mean-field approximation did not lead to a better fit of the experimental data.

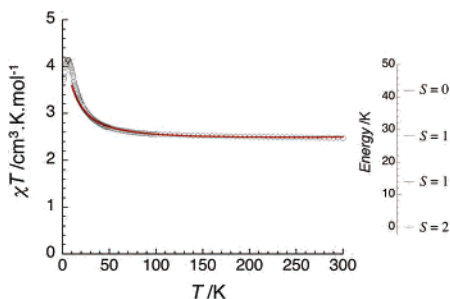


**Figure 2.** Temperature dependence of  $\chi T$  at 1000 Oe (left) and energy level diagram (right) for **3**. Red line: least-squares fitting of the data.

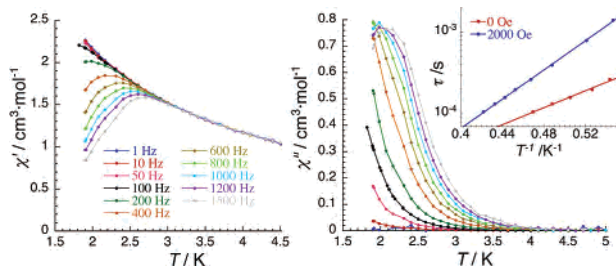


**Figure 3.** Temperature dependence of the real ( $\chi'$ ) and imaginary ( $\chi''$ ) components of the ac susceptibility for **3** ( $H_{dc} = 0$  Oe and  $H_{ac} = 3$  Oe) between 1 and 1500 Hz. Inset:  $\tau$  vs  $T^{-1}$  plot at  $H_{dc} = 0$  and 2000 Oe. The solid lines represent an Arrhenius fit of the data.

mation),<sup>5</sup> suggesting that **2** is not a SMM in the temperature range measured.

The  $\chi T$  vs  $T$  data for **3** suggest that the Fe<sup>III</sup> and Ni<sup>II</sup> centers are also ferromagnetically coupled (Figure 2) because the  $\chi T$  product gradually increases from 2.34 cm<sup>3</sup> K mol<sup>-1</sup> (300 K), reaching a maximum value of 6.01 cm<sup>3</sup> K mol<sup>-1</sup> at 4 K; below 4 K,  $\chi T$  decreases toward a minimum value of 3.60 cm<sup>3</sup> K mol<sup>-1</sup> at 1.84 K. Fitting of the magnetic data for **3** gives  $J_1/k_B = +7.0(2)$  K and  $g_{iso} = 2.31$  (solid line, Figure 2).<sup>10</sup> The magnitude of the magnetic exchange through the cyanide bridges is comparable to those reported for related complexes.<sup>3,6–9</sup> For **3**, the magnitude of  $J_1$  is much larger than that in **2**, suggesting that the linear cyanide bridges afford more efficient superexchange pathways.<sup>3,6,7</sup> Scaling with the value of  $J_1$ , the  $S = 1$  first excited state for **3** is much higher than that for **2**, being ca. 14 K above the  $S = 2$  ground state (Figure 2). Once again the  $M$  vs  $H_{dc}$  data at 1.85 K support this assumption because the magnetization is nearly saturated, reaching 4  $\mu_B$  at 7 T (Figure S8 in the Supporting Information).<sup>5</sup>

The temperature dependence of the ac susceptibility for **3** was measured at several different frequencies at  $H_{dc} = 0$  Oe (Figure 3). The ac susceptibility is strongly frequency-dependent, suggesting that **3** exhibits slow relaxation of the magnetization. From the data shown in Figure 3, the relaxation time,  $\tau$ , can be determined from the maximum of  $\chi''(T)$ .<sup>1</sup> The relaxation time for **3** follows an Arrhenius law with an energy gap of 12.0 K and  $\tau_0 = 4 \times 10^{-7}$  s (inset of Figure 3). As is the case for many SMMs with small spin states,<sup>11</sup> it is likely that the observed energy barrier takes an effective value, resulting from a “short-cut” of the thermal barrier by QTM. In zero field, the  $\pm m_S$  states have the same energy and QTM between these pairs of levels is possible. When a magnetic field is applied, the  $m_S < 0$  and  $m_S > 0$

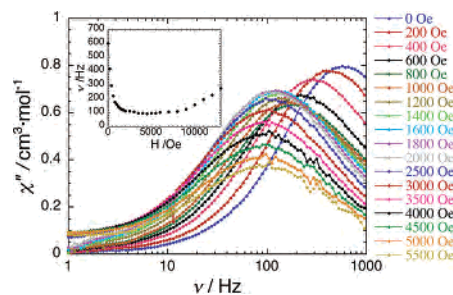


**Figure 4.**  $\chi''$  vs  $\nu$  plot at 1.85 K under various applied  $H_{dc}$  for **3**. Inset: field dependence of the characteristic frequency at 1.85 K.

levels decrease and increase respectively in energy, preventing quantum tunneling between the  $\pm m_S$  states.<sup>1</sup>

To investigate the activated behavior of **3**, we performed ac susceptibility measurements under several applied dc magnetic fields (Figures 4 and S9 and S10 in the Supporting Information).<sup>5</sup> At 1.85 K, the characteristic frequency (maximum of the  $\chi''$  vs  $\nu$  plot) decreases rapidly from 600 Hz at 0 Oe and approaches a nearly constant value of 100 Hz between 2000 and 5000 Oe (inset of Figure 4). As shown by this result, the QTM relaxation pathway remains efficient at 1.85 K.  $\tau$  was thus estimated using the ac data under 2000 Oe (Figure S10 in the Supporting Information). As expected, the relaxation time still follows an Arrhenius law with  $\tau_0 = 2 \times 10^{-8}$  s and an energy gap of 20.6 K is found (inset of Figure 3). It is also worth noting that this energy gap allows for an estimation of the uniaxial anisotropy  $D/k_B \approx -5.2$  K. Finally, the increase of the characteristic frequency (inset of Figure 4) for fields higher than 5000 Oe is expected because resonant QTM should occur for  $H \approx D/g\mu_B \approx 4$  T.<sup>1</sup>

In summary, we have described the syntheses, structures, and magnetic properties of two cyanide-bridged trinuclear Fe<sup>III</sup><sub>2</sub>Ni<sup>II</sup> ( $S = 2$ ) complexes. Magnetic studies suggest that the magnitude of the magnetic exchange between the Fe<sup>III</sup> and Ni<sup>II</sup> centers can be controlled via ancillary ligand choice, and ac susceptibility measurements in a nonzero dc field indicate that **3** is a SMM.

**Acknowledgment.** S.M.H. gratefully acknowledges the donors of the American Chemical Society Petroleum Research Fund (PRF 38388-G3), the Kentucky Science and Engineering Foundation (Grants KSEF-621-RDE-006 and KSEF-992-RDE-008), and the University of Kentucky Summer Faculty Research Fellow and Major Research Project programs for financial support. R.C. thanks MAGMANet (Grant NMP3-CT-2005-515767), CNRS, Bordeaux 1 University, and the Conseil Régional d'Aquitaine for financial support. G.T.Y. thanks the National Science Foundation (Grant CHE-0210395) for partial financial support.

**Supporting Information Available:** X-ray crystallographic data in CIF format, experimental details, and additional magnetic data. This material is available free of charge via the Internet at <http://pubs.acs.org>.

IC060379B

(11) For pertinent examples, see: Miyasaka, H.; Clérac, R.; Wernsdorfer, W.; Lecren, L.; Bonhomme, C.; Sugiura, K.-I.; Yamashita, M. *Angew. Chem.* **2004**, *116*, 2861–2865.